Available online at www.eccomasproceedia.org
Eccomas Proceedia COMPDYN (2025) 42 5-4244

ECCOMAS
Proceedia

COMPDYN 2025
10th ECCOMAS Thematic Conference on
Computational Methods in Structural Dynamics and Earthquake Engineering
M. Papadrakakis, M. Fragiadakis (eds.)
Rhodes Island, Greece, 15-18 June 2025

PRELIMINARY OPENSEES MODELING TO PREDICT CYCLIC BEHAVIOUR OF ALUMINUM SHS BEAMS

Maria Maglio[1], Elide Nastri[1], Alessandro Pisapia[2], Francesco Pisciottano[1], Evangelia Georgantzia[3]

[1]University of Salerno
Dept. Civil Engineering, Italy

[2]Pegaso Telematic University
Dept. Engineering, Italy

[3] City St George's, University of London
Northampton Square, London EC1V 0HB, United Kingdom

e-mail: mamaglio@unsa.it, enastri@unisa.it,
alessandro.pisapia@unipegaso.it, fpisciottano@unisa.it, evangelia.georgantzia@city.ac.uk

Abstract

The use of aluminium alloys in structural applications has gained significant attention due to their high strength-to-weight ratio, corrosion resistance, and sustainability. This study investigates the cyclic behavior of Square Hollow Section (SHS) beams made from 6060-T66 aluminium alloy by comparing experimental testing and numerical modeling. Building on the experimental campaign provided in the scientific literature, which analyzed the response of SHS beams under cyclic bending, this research develops a numerical model in OpenSees to simulate cyclic degradation. The model employs the Giuffrè-Menegotto-Pinto constitutive material in conjunction with the Fatigue Material. Calibration was performed using experimental data, adjusting key parameters to accurately replicate force-displacement curves and total dissipated energy. The results demonstrate that, with appropriate calibration, the proposed modeling approach reasonably reflects the cyclic response observed in the experimental tests, including material degradation due to cyclic loading. A relationship between the width of the fatigue material application region and the internal plate width was also established. This study provides valuable insights into the structural design of aluminium elements subjected to cyclic loading, contributing to the advancement of aluminium-based structural systems.

Keywords: Aluminium Alloys, Cyclic Behavior, Fatigue Material, OpenSees, Numerical Modeling, Fiber Element Modeling.

doi: 10.7712/120125.127 1.25287

1 INTRODUCTION

Aluminium alloys have garnered increasing attention in structural engineering due to their favorable properties, such as high strength-to-weight ratios, excellent corrosion resistance, and overall sustainability. These advantages make aluminium a promising material for a variety of applications, ranging from lightweight roofing and offshore structures to mobile bridges [1],[2]. In particular, the 6xxx and 7xxx series aluminium alloys are widely used in structural applications, with the 6060-T66 alloy standing out due to its balanced combination of strength, ductility, and formability [3]. As structural applications of aluminium alloys continue to grow, understanding their performance under cyclic loading becomes critical [4], especially for elements that may be subjected to repeated stresses, such as beams and frames.

To date, only a limited number of research studies are available on the cyclic behaviour of aluminium alloy members, while most concern simple uniaxial cyclic behaviour. Among the first is that of Hopperstad et al.[5] in which material characteristics such as the shape of the hysteresis loops, cyclic hardening and softening are deduced for alloy AA6060-T4 and T6. Guo et al.[6] conducted different cyclic loading cases for the 6082-T6 and 7020-T6 alloys analysing their hysteretic response and proposing a uniaxial hysteretic constitutive model. More recently, Pisapia et al.[7] conducted an extensive experimental campaign analysing five alloys belonging to the 5xxx, 6xxx and 7xxx series under both monotonic and cyclic conditions and evaluated their cyclic hardening/softening effects, the main mechanical parameters and the low cycle fatigue curves. Georgantzia et al [8], performed low-cycle high amplitude fatigue tests for 6082-T6, 6063 T6 and 6060-T5 aluminium alloys exploiting the results to calibrate a low-cycle fatigue life model.

This study builds upon an experimental campaign conducted by Nastri et al. [9] , which examined the cyclic behavior of Square Hollow Section (SHS) beams made from 6060-T66 aluminium alloy with different width-to-thickness ratios, affected by local buckling phenomena and cyclic degradation due to non-uniform bending stresses. To simulate these phenomena, in this work a numerical model was developed using OpenSees software, an advanced computational framework for nonlinear analysis of structural systems [10]. The *Giuffrè-Menegotto-Pinto* material model [11], commonly used for capturing the cyclic behaviour of materials, was integrated with a *Fatigue Material* command to simulate degradation due to cyclic loading. Georgantzia et al. previously developed a fiber element model in OpenSees, employing a modified *Giuffrè–Menegotto–Pinto* model to analyze the flexural buckling performance of 6082-T6 aluminium alloy columns [4].

By comparing experimental results with the predictions of the calibrated numerical model, this paper aims to contribute to a better understanding of the cyclic response of aluminium beams and improve the design methods for aluminium elements subjected to cyclic loading.

It is important to emphasize that this study represents a preliminary approach for developing a numerical model that incorporates the *Giuffrè-Menegotto-Pinto* material model along with the *Fatigue Material* command. While the model successfully captures the experimental results and simulates the cyclic behavior of aluminium SHS beams with reasonable accuracy, further work is necessary to refine and calibrate the cyclic parameters. The goal is to enhance the model’s accuracy, ensuring it can more precisely predict the behaviour of aluminium structures under cyclic loading in future applications.

2 PREVIOUS EXPERIMENTAL CAMPAIGN

The experimental campaign conducted by Nastri et al. [9] investigated the behavior of SHS beams made from 6060-T66 aluminium alloy. This alloy is widely used in structural applications due to its excellent corrosion resistance and suitability for extrusion into complex profiles. Further details on its chemical composition and mechanical properties can be found in [9]. Four different cross-sections, *SHS40*, *SHS60*, *SHS80*, and *SHS100* were teste at the University of Salerno, each with two distinct lengths (1300 mm and 1000 mm), resulting in a total of eight beam specimens. These specimens were subjected to three-point cyclic bending tests, with incremental displacement applied at midspan. The loading test setup is illustrated in Figure 1a.

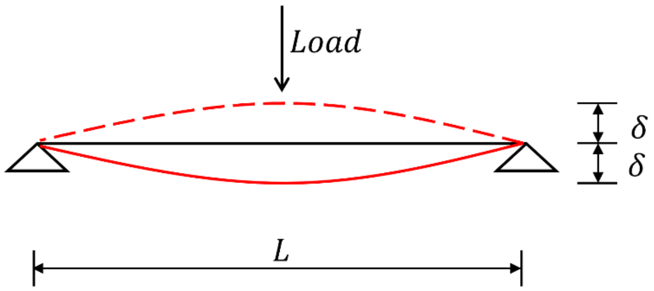

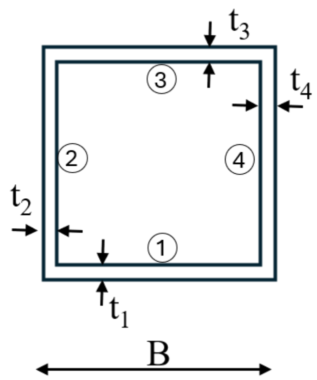

Figure 1: a) Scheme of Loading Test. b) Cross-Section Geometry.

This study focuses exclusively on beams with a length of 1300 mm. Their geometric properties, referenced in Figure 1b, are summarized in Table 1. According to the current EN 1999-1-1 standard [12], all tested sections belong to Class 4, except for *SHS40*, which is classified as Class 2. Consequently, the primary failure mode observed was local buckling at the beam's midspan, where the bending moment reaches its maximum. This failure mechanism is clearly visible in the post-test images of the specimens presented in the original work [9].

Specimen	L [mm]	B [mm]	t_1 [mm]	t_2 [mm]	t_3 [mm]	t_4 [mm]
SHS 40_L1	1300	40	2.10	2.40	2.02	1.99
SHS 60_L1	1300	60	2.16	2.10	2.06	2.13
SHS 80_L1	1300	80	2.06	2.10	2.00	1.98
SHS 100_L1	1300	100	2.13	2.00	2.30	2.33

Table 1: Geometric Properties of Tested Beams.

3 NUMERICAL MODEL IMPLEMENTATION

To simulate the cyclic response of aluminium SHS beams, the computational framework OpenSees was employed [10]. OpenSees provides various modeling options for beam-column members, allowing for an efficient and accurate representation of their behaviour under cyclic loading. In this study, to simulate the behaviour of 6060 aluminium alloy beams under cyclic loading, as well as the degradation in the central section where the load is applied, the specimen was divided into four elements.

- Two *Elastic Beam-Column elements* were assigned to the outer regions, away from the load application points (ele.1 and ele.4).

- Two *Nonlinear Beam-Column elements* with fiber discretization, that allows the spread of plasticity along them for the midspan section (ele.2 and ele.3), with a total length equal to 200mm, to be sure to cover the area where material degradation occurs. As shown in Figure 4c, each plate of the cross-section was divided into 28 segments along the width and 4 elements along the thickness, resulting in a total of 448 fibers over the cross-section.

Figure 2 illustrates the numerical model, highlighting the different element types used. To ensure computational efficiency, only two nonlinear Beam-Column elements are located at midspan, but with an increased number of *integration points* (in this case 7). This approach significantly reduces computational costs while still maintaining high accuracy in capturing the nonlinear response of the beams.

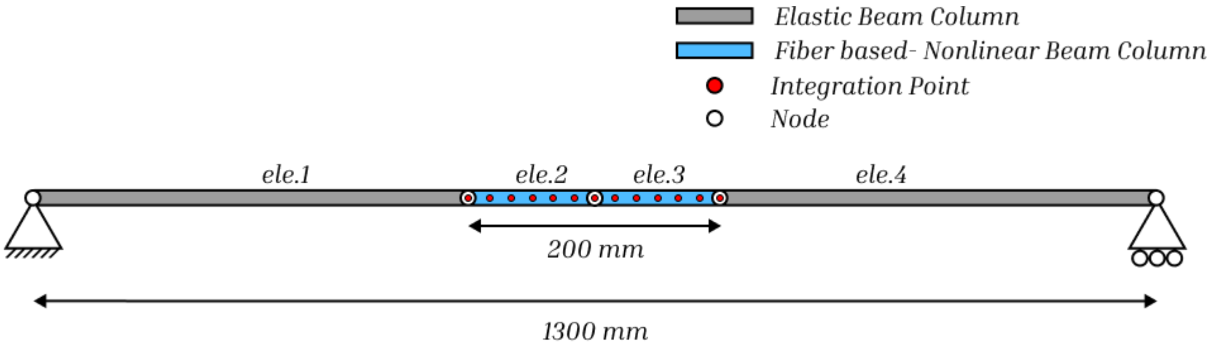

Figure 2: Numerical model scheme.

However, with this type of element, local buckling and section distortion cannot be directly accounted for, as it is assumed that plane sections conserve the planarity. To address this limitation, a fiber removal technique was adopted, utilizing the *fatigue material* command implemented in OpenSees. This command, originally conceived to simulate the effects of low-cycle fatigue, was calibrated appropriately to model material degradation due to cyclic loading. A similar approach has been successfully applied in previous studies [13],[14].

The uniaxial *Giuffrè-Menegotto-Pinto* material model [11], implemented using the Steel02 material command in OpenSees, was assigned to the cross-section fibers. This model allows for yielding, the Baushinger effect, as well as kinematic and isotropic hardening responses through 10 parameters: E_0, $\sigma_{0.2}$, b, R_0, cR_1, cR_2, α_1, α_2, α_3, and α_4. E_0 is the initial Young's modulus; $\sigma_{0.2}$ is the yield stress; b is the post-yield hardening ratio; R_0 is the initial curvature; cR_1 and cR_2 are the curvature variation parameters of the Bauschinger curve after each strain reversal; α_1, α_2, α_3, and α_4 are the isotropic hardening parameters in compression and tension. The first four parameters were calibrated based on the true stress-true strain curves from the monotonic tensile tests available in [9]. The comparison between the numerical model and experimental results can be seen in Figure 3.The remaining parameters, which characterize the nonlinear response under cyclic loading, were taken from the values recommended by Georgantzia et al. [4] based on their cyclic coupon tests on 6000 series aluminium alloys. The parameters values used for each cross-section are listed in Table 2.

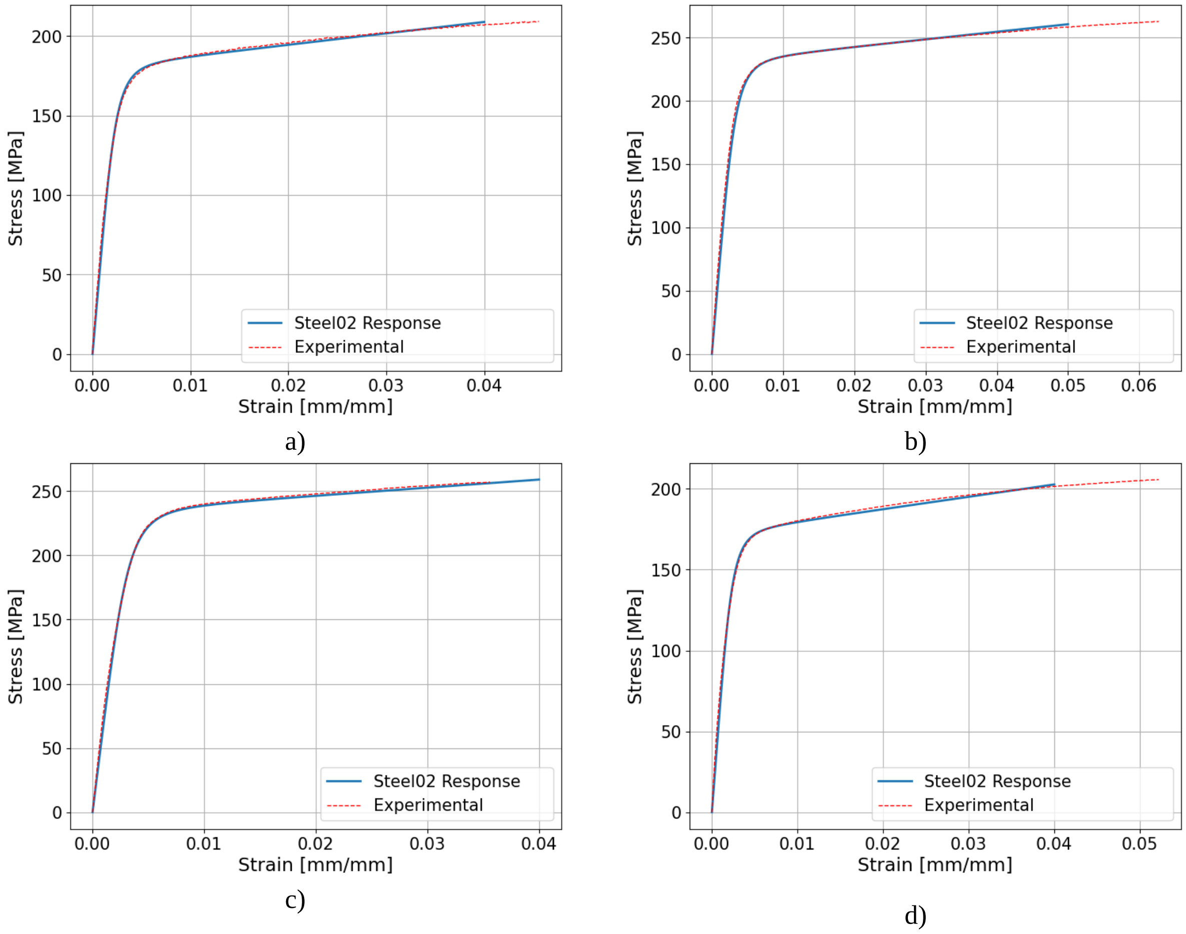

Figure 3: Comparison of Experimental and Numerical Monotonic Stress-Strain Curves: a) SHS40 specimen, b) SHS60 specimen, c) SHS60 specimen, d) SHS100 specimen.

Specimen	$\boldsymbol{E_0}$	$\boldsymbol{\sigma_{0.2}}$	$\boldsymbol{b}$	$\boldsymbol{R_0}$	$\boldsymbol{cR_1}$	$\boldsymbol{cR_2}$	$\boldsymbol{\alpha_1}$	$\boldsymbol{\alpha_2}$	$\boldsymbol{\alpha_3}$	$\boldsymbol{\alpha_4}$
SHS40	71769	238	0.010	3.5	0.6	0.15	0.046	1.0	0.021	1.0
SHS60	66218	240	0.010	3.5	0.6	0.15	0.046	1.0	0.021	1.0
SHS80	71769	190	0.010	3.5	0.6	0.15	0.046	1.0	0.021	1.0
SHS100	69458	174	0.010	3.5	0.6	0.15	0.046	1.0	0.021	1.0

Table 2: Steel02 Model Parameters.

As anticipated to account for material degradation caused by low-cycle fatigue, the *Fatigue Material* command was applied to a portion of the fiber section. This command wraps around the *Steel02* material model and does not influence its stress-strain response until the Damage Index reaches a value of 1.0, causing the strength of the main material (*Steel02*) to drop to zero. The cumulated damage in each cycle is computed using a linear strain accumulation model beased on Miner's Rule, incorporating a modified rainflow cycle counting method proposed by Uriz [15]. This method evaluates only the four most recent strain reversal peaks, ensuring computational efficiency while maintaining accuracy. The two main parameters defining the fatigue model are:

- *m* (*Fatigue Ductility Exponent*), representing the slope of the log-log relationship between plastic strain amplitude ($\Delta\varepsilon$) and the number of cycles to failure (N_f).

- ε_0 (*Fatigue Ductility Coefficient*), representing the plastic strain level at which a single cycle results in failure [10].

These parameters were calibrated directly by comparing numerical hysteretic curves with experimental data.

The main goal is to avoid the premature collapse due to simultaneous fiber failure. In fact, a direct application of the *Fatigue Material* command to all fibers in the upper and lower flanges would lead to simultaneous strength degradation across these fibers, causing a sudden loss of load-carrying capacity and premature section failure. To mitigate this issue, the *Fatigue Material* command was applied only to a calibrated portion (l_f), of each plate, where l_f is defined as a function of the internal width (b) of the plate.

As an example, a comparison of the force-displacement curves for SHS60 beam without the use of the *Fatigue Material*, with the use of the *Fatigue Material* model applied to the entire cross-section and with the *Fatigue Material* model applied to a calibrated width (l_f) of the section is shown in Figure 4 (a,b,c).

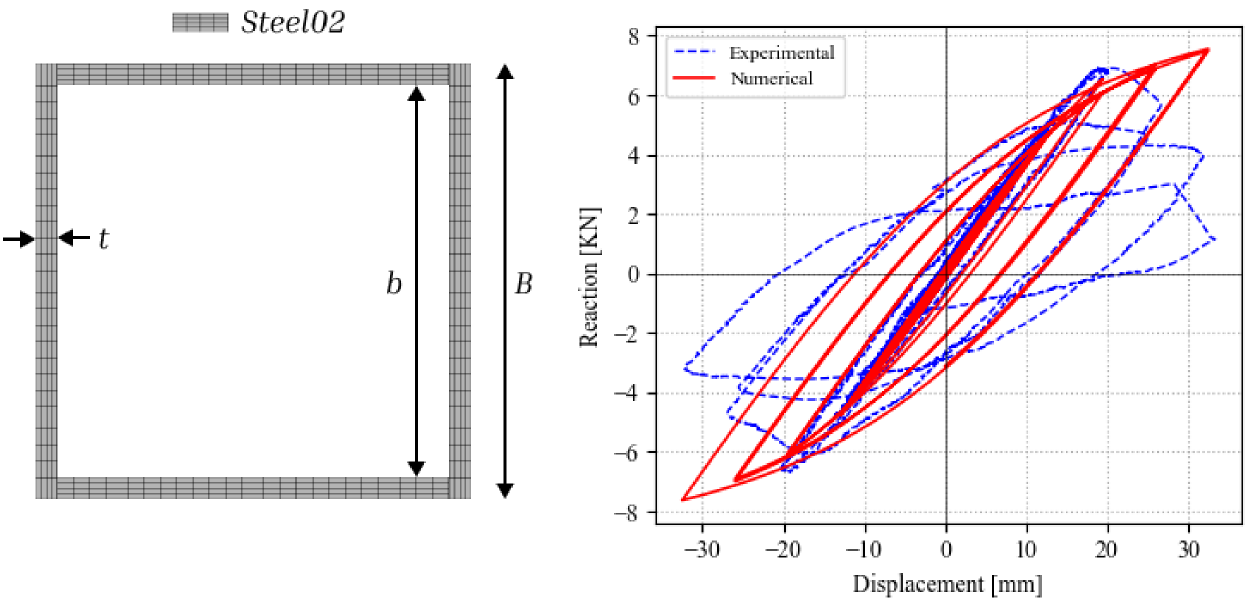

a)

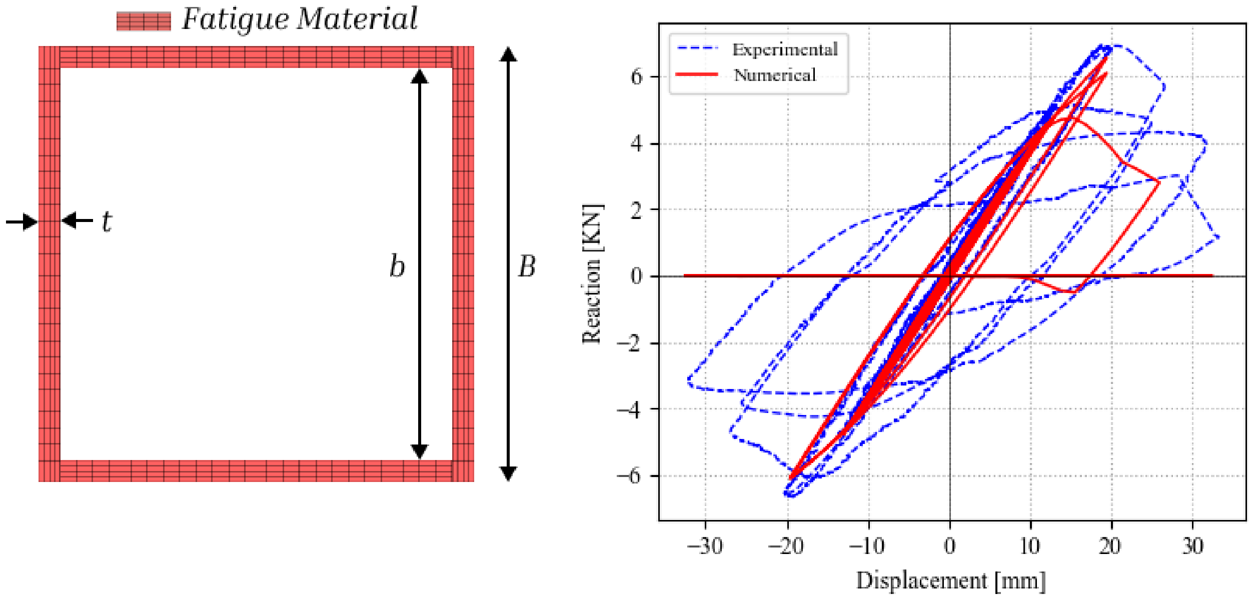

b)

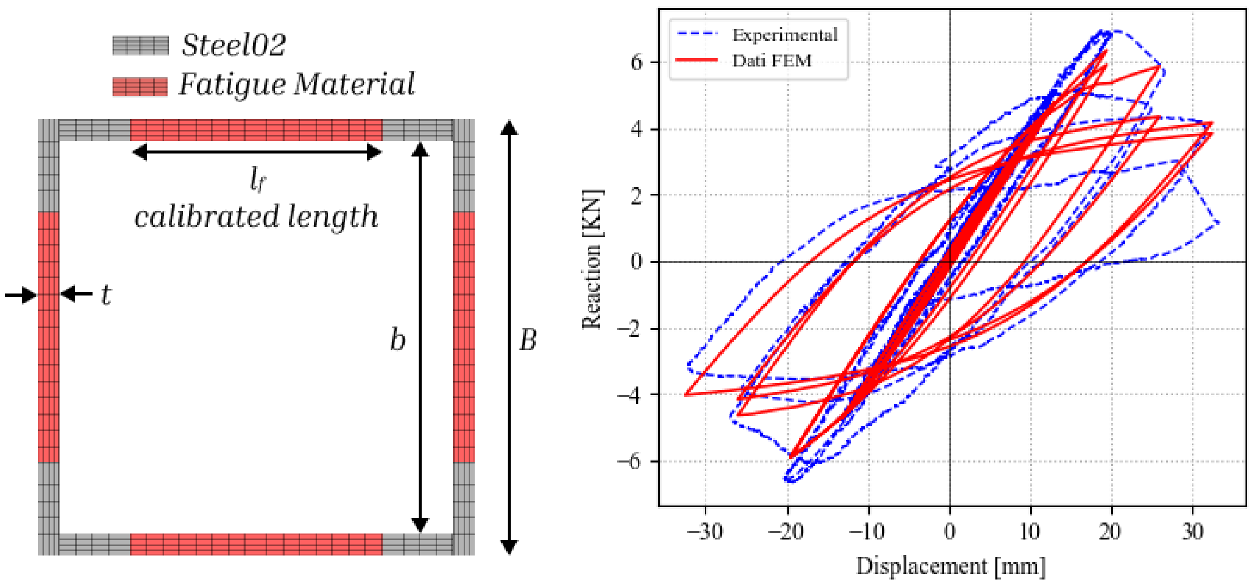

c)

Figure 4 .Comparison of force-displacement curves for the SHS60 beam under three conditions: (a) without the fatigue material model, (b) with the fatigue material model applied to the entire cross-section, and (c) with the fatigue material model applied to a calibrated portion of the section

4 MODEL CALIBRATION AND RESULTS

The calibrated values of ε_0, m, and the width of the region with the fatigue material l_f for the different cross-sections are presented in Table 3. A comparison of the force-displacement curves between the experimental tests and the calibrated OpenSees model is shown in Figure 5, proving that the numerical model successfully captured the main characteristics of the experimental hysteretic response, including stiffness degradation and strength reduction due to cyclic loading. Additionally, Figure 6 illustrates the comparison of the total energy dissipated, calculated as the cumulative area under the force-displacement curve for each cycle. The results demonstrate that, with proper calibration, the *Fatigue Material* command in OpenSees can effectively simulate cyclic degradation due to local bucking. Notably, the *Fatigue Ductility Exponent* (m) remains consistent across Class 4 sections (SHS60, SHS80, SHS100). This consistency allowed for the derivation of a relationship between l_f and the plate width (b) as depicted in Table 3. It is important to highlight that this calibration is validated only for sections with a constant 2 mm thickness and classified as slender (Class 4).

Specimen	ε_0	**m**	l_f
SHS 40	0.168	-1.0	0.50b
SHS 60	0.168	-1.28	0.70b
SHS 80	0.168	-1.28	0.85b
SHS 100	0.168	-1.28	0.88b

Table 3: Calibrated Fatigue Material Parameters.

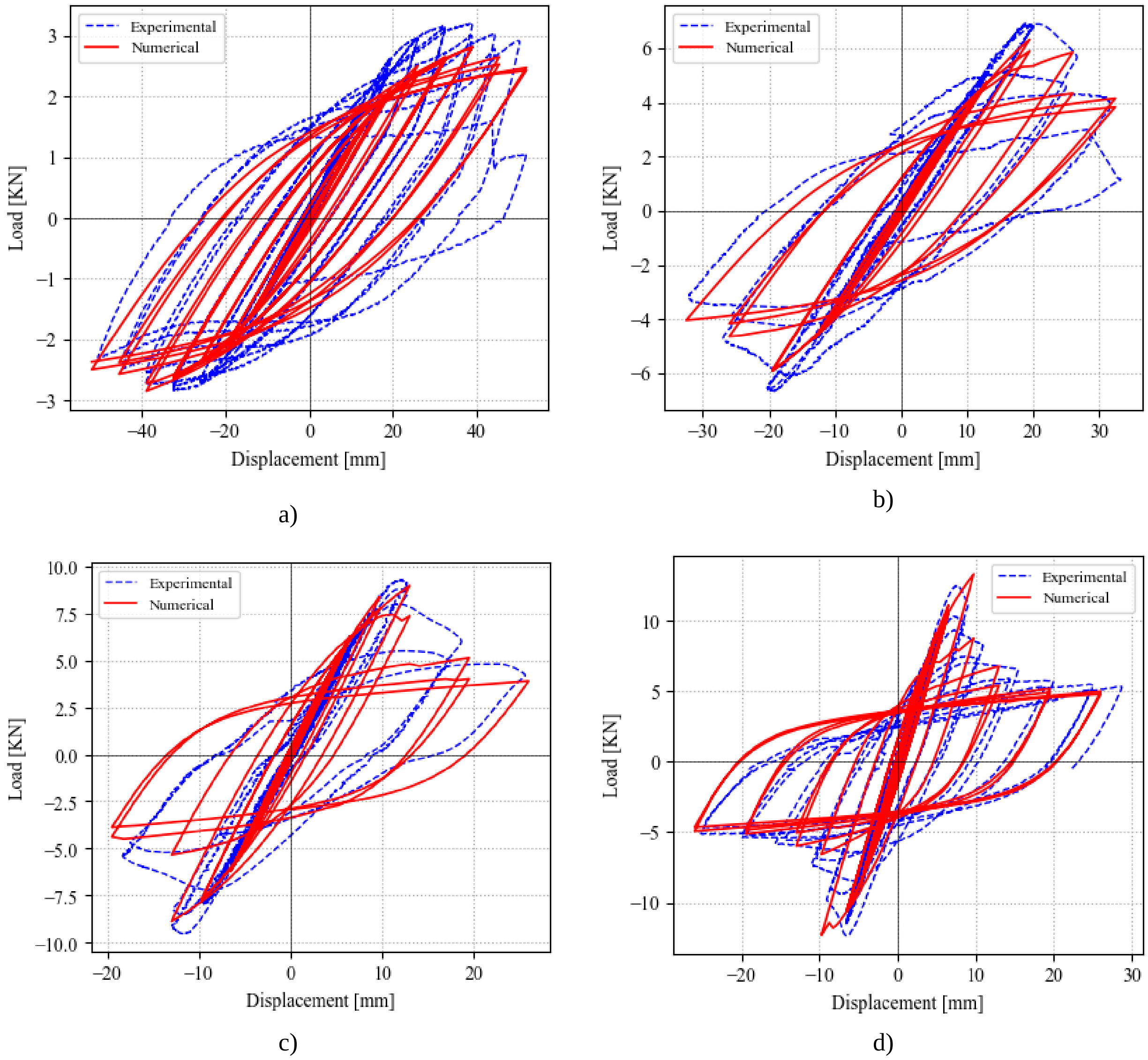

Figure 5: Comparison of Force-Displacement curves between experimental and numerical results for different SHS specimens: (a) SHS40, (b) SHS60, (c) SHS80, and (d) SHS100.

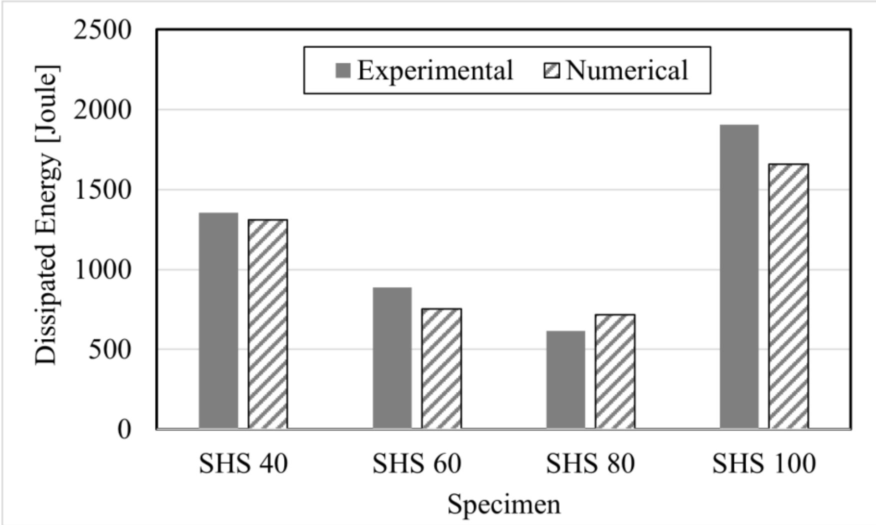

Figure 6: Comparison of total dissipated energy between experimental and numerical results.

5 CONCLUSIONS AND FUTURE DEVELOPMENTS

- This study presents a numerical approach for simulating the cyclic behaviour of SHS aluminium beams, accounting for material degradation due to low-cycle fatigue using the *Fatigue Material* model in OpenSees. The model was developed with a combination of elastic and nonlinear beam-column elements with fiber discretization.
- The *Giuffrè-Menegotto-Pinto* material model (Steel02), calibrated through stress-strain curves from experimental tensile test, was used to account for the cyclic behaviour of the 6060-T66 aluminium alloy. To replicate the material degradation caused by low-cycle fatigue, the *Fatigue Material* command was applied to select fibers within the cross-section. The fatigue parameters ε_0 and m were calibrated through comparison with experimental hysteretic curves.
- The calibration results demonstrated that applying the *Fatigue Material* to a controlled region (l_f), rather than the entire section, provided a realistic representation of the cyclic degradation, allowing the application of the proposed approach to similar aluminium sections with comparable geometries and thickness.
- The comparison of total dissipated energy further confirmed the model's ability to replicate the cyclic performance of aluminium beams, with a difference of 3.17%, 15.26% and 13.01% for SHS40, SHS60 and SHS100 beams respectively, and an overestimation compared to experimental tests of 16.2% only in the case of the SHS80 beam.
- While the proposed model effectively simulates the structural response under cyclic loading, further research is required to account for local buckling and extend its applicability to sections with varying thicknesses and different loading conditions.
- Future efforts will focus on calibrating the parameters related to the cyclic behavior in the *Giuffrè-Menegotto-Pinto* model, which are crucial for improving the model's accuracy in simulating the cyclic response of aluminium structures.
- By refining the calibration of parameters such as α_1, α_2, α_3, α_4, cR_1, and cR_2, the objective will be to achieve a more precise representation of the structural behavior under cyclic loading conditions. This will enhance the overall predictive capabilities of the model, leading to a more accurate simulation of aluminium structures subjected to cyclic stresses.

REFERENCES

[1] F.M. Mazzolani, 3D aluminium structures. *Thin-Walled Structures*, **61**, 258–266, 2012.

[2] E. Georgantzia, M. Gkantou, G.S. Kamaris, Aluminium alloys as structural material: A review of research. *Engineering Structures,* **227**, art. no. 111372, 2021.

[3] J.G. Kauffman, Introduction to Aluminum Alloys and Tempers. *ASM International*, 2000.

[4] E. Georgantzia, C. Finney, A.F. Robinson, M. Kashani, Modeling Nonlinear Stress–Strain Behavior of 6000 Series Aluminum Alloys under Cyclic Loading. *Journal of Materials in Civil Engineering*, **36**, 2024.

[5] O.S. Hopperstad, M. Langseth, S. Remseth: "Cyclic stress-strain behaviour of alloy AA6060, Part I: Uniaxial experiments and modelling". *International Journal of Plasticity*, **11**(6), pp. 725-39, 1995.

[6] X. Guo, L. Wang, Z. Shen, J. Zou, L. Liu: "Constitutive model of structural aluminium alloy under cycling loading", Construction and Building Materials, 180, pp. 643-654, 2018.

[7] A. Pisapia, E. Nastri, V. Piluso, A. Formisano, F.M. Mazzolani, Experimental campaign on structural aluminium alloys under monotonic and cyclic loading. *Engineering Structures*, **282**, 2023.

[8] E. Georgantzia, P.J. Vardanega, M.M. Kashani, Modelling low-cycle fatigue behaviour of structural aluminium alloys. *Bulletin of Earthquake Engineering*, 2025.

[9] E. Nastri, V. Piluso, A. Pisapia, F. Pisciottano, P. Todisco, First exploring the cyclic behaviour of aluminium beams under non-uniform bending: Experimental and FE analysis. *Engineering Structures*, **322**, Part B, 2025.

[10] S. Mazzoni, F. McKenna, M.H. Scott, G.L. Fenves, B. Jeremic, OpenSees Command Language Manual. *Pacific Earthquake Engineering Research Center, University of California at Berkeley*, 2003.

[11] F. Giuffrè, P. Menegotto, M. Pinto, Mathematical model for the cyclic behavior of steel materials. Open System for Earthquake Engineering Simulation (OpenSees), *Pacific Earthquake Engineering Research Center, University of California, Berkeley*, 2000.

[12] CEN (European Committee for Standardization), Eurocode 9: Design of Aluminium Structures – Part 1-1: General Structural Rules. *EN 1999-1-1, Brussels*, 2007.

[13] M. Bosco, L. Tirca, Numerical simulation of steel I-shaped beams using a fiber-based damage accumulation model. *Journal of Constructional Steel Research*, **133**, 2017.

[14] B. Hariri, R. Tremblay, Influence of flange local buckling of I-shaped braces on the seismic response of concentrically steel braced frames. *17^{th} World Conference on Earthquake Engineering*, 2021.

[15] P. Uriz, Towards earthquake resistant design of concentrically braced steel buildings. Department of Civil and Environmental Engineering, University of California, Berkeley, 2005.